

Lanthanum titanate ceramics: Electrical characterizations in large temperature and frequency ranges

D. Fasquelle^{a,*}, J.C. Carru^a, L. Le Gendre^b, C. Le Paven^b,
J. Pinel^b, F. Chevire^c, F. Tessier^c, R. Marchand^c

^a LEMCEL, Université du Littoral Côte d'Opale, 50, rue Ferdinand Buisson, B.P. 717, 62228 Calais, Cedex, France

^b I.U.T. de St-Brieuc, IETR, UMR-CNRS 6164, Université de Rennes 1, France

^c Laboratoire "Verres et Céramiques", UMR-CNRS 6512, Inst. Ch. Rennes, Université de Rennes 1, France

Available online 1 April 2005

Abstract

Ceramics of the $\text{La}_2\text{O}_3\text{-TiO}_2$ system have very good dielectric properties, which make $\text{La}_2\text{Ti}_2\text{O}_7$ a good candidate for microwave applications. Using radio-frequency magnetron sputtering, we have deposited LaTiO_xN_y oxynitride thin films on (001) strontium titanate and glass substrates, starting from a homemade oxide target. The microwave dielectric properties of $\text{La}_2\text{Ti}_2\text{O}_7$ ceramic have been investigated in the 100 Hz to 10 GHz range in order to have a reference for further studies. The evolution of ϵ' and ϵ'' shows a space charge domain with a critical frequency $F_c = 1$ GHz. Measurements in the temperature range from 20 to 880 °C have been carried out to study phase transitions and conduction mechanisms.

© 2005 Elsevier Ltd. All rights reserved.

Keywords: Sintering; Dielectric properties; Impedance; Ionic conductivity; Perovskite

1. Introduction

$\text{La}_2\text{Ti}_2\text{O}_7$ perovskite is a ferroelectric ceramic, which has already been synthesized as single crystal. It then presents high electro-optical and piezoelectric properties,¹ and remains ferroelectric up to the temperature of 1500 °C.² Its very high Curie temperature defines it in fact as one of the best candidates for high temperatures applications. Ceramics of the $\text{La}_2\text{O}_3\text{-TiO}_2$ system have also very good dielectric properties such as a low temperature coefficient of permittivity, weak losses at medium frequencies (100 kHz–1 MHz),³ which make $\text{La}_2\text{Ti}_2\text{O}_7$ a good candidate for microwave applications. Some measurements on resonators have already been made at about 10 GHz.⁴ More recently, thin films deposition has allowed to make electronic devices like ferroelectric grid FET, tunable filters or antennas. Using radio-frequency (r_f) magnetron sputtering, we have deposited LaTiO_xN_y oxynitride thin films on (001) strontium

titanate and glass substrates, starting from a homemade oxide target.⁵

In this paper, the microwave dielectric properties of $\text{La}_2\text{Ti}_2\text{O}_7$ ceramic have been investigated in order to have a reference for further studies. These results are presented in extended ranges, to our knowledge, for the first time. The behaviour of this ceramic is also presented in a large temperature range.

2. Experimental details

2.1. Powder synthesis

$\text{La}_2\text{Ti}_2\text{O}_7$ powder was prepared by molten salt synthesis.⁶ La_2O_3 and TiO_2 precursors were mixed in a 1:2 mole ratio. A salt consisting of 50 mol% NaCl/50 mol% KCl was then added, constituting 50 wt.% of the total reaction mixture. The corresponding mixture was heated at 1000 °C for 15 h. The resulting product was washed using distilled water and clearly identified, as $\text{La}_2\text{Ti}_2\text{O}_7$, by X-ray diffraction.

* Corresponding author. Tel.: +33 321465778; fax: +33 321465778.

E-mail address: didier.fasquelle@univ-littoral.fr (D. Fasquelle).

2.2. Dielectric properties measurement

Small dense oxide pellets ($\varnothing=3$ mm) were prepared by pressure-less sintering at 1400 °C for 3 h under air. Gold–palladium electrodes were sputtered on either side of the sintered pellets. The following devices have been used: a HP4284A LCR bridge from 20 Hz to 1 MHz, a HP4291A LCR bridge from 1 MHz to 1.8 GHz and an ANRITSU 37369A vectorial analyser from 40 MHz to 40 GHz. We have made a specific support for the pellets which can be used with all our measurement systems. The following parameters were measured: ϵ' (permittivity), ϵ'' (losses), $\text{tg } \delta$ (loss tangent), σ_{ac} (ac conductivity) and have been described earlier.⁷

3. Results and discussion

3.1. Microwaves dielectric measurements

Fig. 1 represents the permittivity ϵ' and the loss tangent $\text{tg } \delta$ as function of frequency in the range 100 Hz–10 GHz. The ϵ' value is about 57 up to 100 MHz. On other pellets, we have measured values comprised between 48 and 50. These values are close to those mentioned in the literature which lie between 45 and 54.^{4,6} The difference can be related to the temperature of synthesis of the powders, the density after forging, and the conditions of annealing. Below 500 Hz, the resistance of the samples is too high to be correctly measured by the impedance bridge, which does not allow us to give values of $\text{tg } \delta$ in this range. The values obtained in the various ranges of measurement correctly overlap, which validates the procedures of calibration of the two impedance bridges and the vectorial analyser.

Above 200 MHz, an important decrease of ϵ' is observed, which lets us think of the existence of a relaxation domain. The loss tangent remains lower than 0.01 up to 50 MHz with intermediate values, which are: 1.6×10^{-3} at 100 kHz and 2.75×10^{-3} at 10 MHz. Above 10 MHz the strong increase of $\text{tg } \delta$ can be due to a relaxation domain, but other investiga-

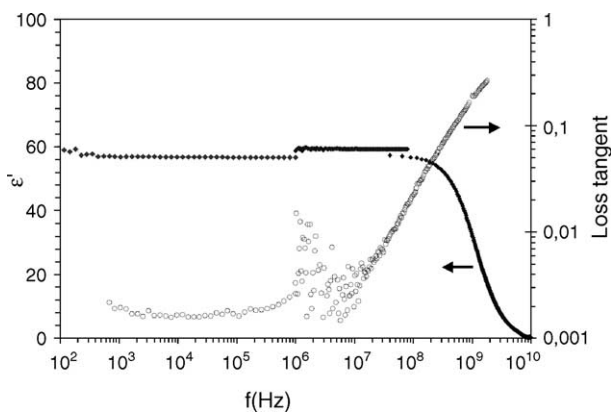


Fig. 1. Dielectric measurements vs. frequency: permittivity ϵ' and loss tangent $\text{tg } \delta$ (log scale) at room temperature.

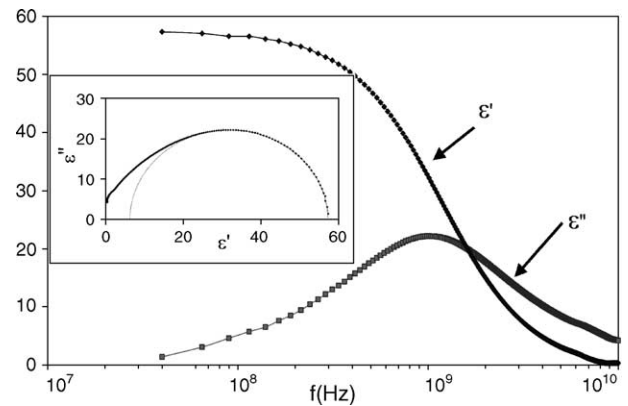


Fig. 2. Relaxation domain observed on plots of the losses and the permittivity in the 10 MHz to 10 GHz frequency range, at room temperature. On the inset, the diagram of Argand $\epsilon''(\epsilon')$ is given.

tions on ferroelectric materials have shown the same evolution in the 1 MHz to 10 GHz frequency range.⁸ So it can be dependent on the ferroelectric structure because the evolution of $\text{tg } \delta$ follows the one of the ac conductivity.

The relaxation domain is observed by plotting ϵ' and ϵ'' versus frequency or an Argand's diagram $\epsilon''(\epsilon')$ as shown on Fig. 2.

Fig. 2 shows a critical frequency $F_c = 1$ GHz. The diagram of Argand (Fig. 2) has an asymmetrical form, which is the characteristic of a Davidson–Cole type domain.

Complementary measurements were carried out to check the existence of a relaxation domain beyond 200 MHz by heating the sample. The relaxation domain has shown a dependence on the temperature. It shifts in higher frequency with increasing temperature and its amplitude increases too. We have calculated its activation energy: $E_a = 0.1$ eV. This value is quite the same as the dc conductivity one. This result highlights the relaxation is not due to a dipolar relaxation but to an accumulation of free carriers at the electrodes, which entails the creation of a space charge. This phenomenon has also been observed on titanates.⁹

3.2. Dielectric measurements in the 20–880 °C temperature range

The evolution of the permittivity ϵ' is presented in Fig. 3. ϵ' is practically constant from room temperature to 280 °C. Beyond this temperature, the behaviour of ϵ' strongly depends on the frequency. At 1 kHz, the dielectric permittivity varies from 57 at room temperature to 5500 at 880 °C. There is no maximum reached in the range. Indeed, the Curie temperature of $\text{La}_2\text{Ti}_2\text{O}_7$ is 1500 °C (1773 K).²

Fig. 4 presents the dielectric losses according to the temperature. Two plateaus are remarkable on these curves. The first is at 650 K (377 °C), the second starting from 1100 K (827 °C). These behaviours, which can be seen at different frequencies, are usually associated with a phase transition. Raman spectra of $\text{La}_2\text{Ti}_2\text{O}_7$ obtained at various temperatures have shown an asymmetry of the peak starting from

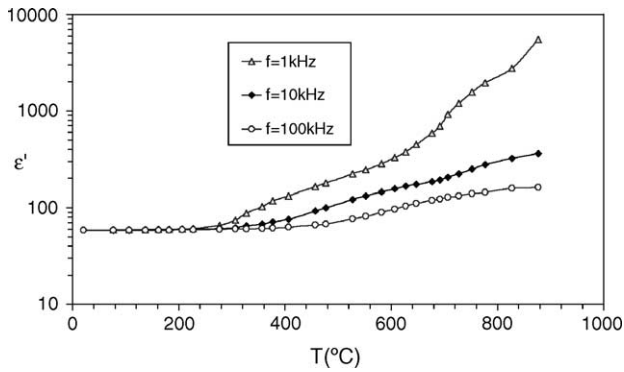


Fig. 3. Dielectric permittivity measured at three frequencies (1, 10 and 100 kHz). ϵ' is given with a logarithmic scale.

572 K¹⁰ (299 °C). Therefore, the plateau observed between 320 and 400 °C is thus perhaps in relation with a slight distortion of the perovskite cell: slight shift of Ti ions modifying the electrostatic effect with the oxygen octahedron, and this implying a modification in the conduction regime of the ceramic. At 827 °C (1100 K), we observe the beginning of a phase transition because the La₂Ti₂O₇ ceramic passes from the monoclinic phase to the orthorhombic phase. This phase is preserved up to 1500 °C, temperature from which it will be in the paraelectric state. Indeed, Nanamatsu et al.^{1,2} have found that the monoclinic phase becomes orthorhombic beyond 780 °C (1053 K).

The ac conductivity, given Fig. 5, presents a large variation from 2×10^{-8} S/m (room temperature) to 8×10^{-3} S/m (880 °C) for a frequency of 1 kHz. The change in slope near 377 °C is in relation with the same behaviour in ϵ'' plots. At this temperature, the ceramic is in the monoclinic phase, so this behaviour at the various frequencies is probably due to an electrostatic effect between the oxygen octahedron and the Ti ion, which induces a distortion of the perovskite cell.

On this same figure, we have also plotted straight lines obtained for various activation energies with the equation: $\sigma(T) = \sigma_0 \times \exp(-E_a/k_B T)$ where σ_0 is a constant; E_a is the activation energy and T the temperature. At temperatures below 230 °C, the very weak slope gives an energy $E_{a1} = 0.04$ eV for $f = 100$ kHz ($E_{a2} = 0.1$ eV at 1 kHz). This

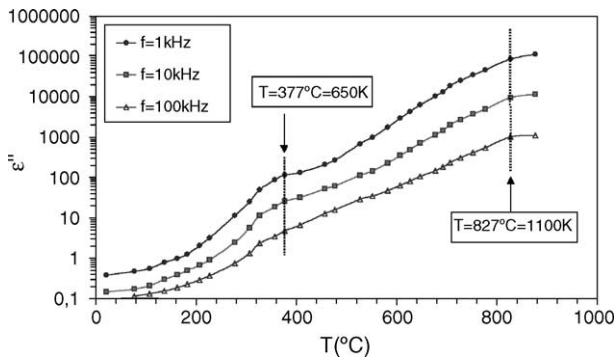


Fig. 4. Dielectric losses at three frequencies (1, 10 and 100 kHz). ϵ'' is given with a logarithmic scale.

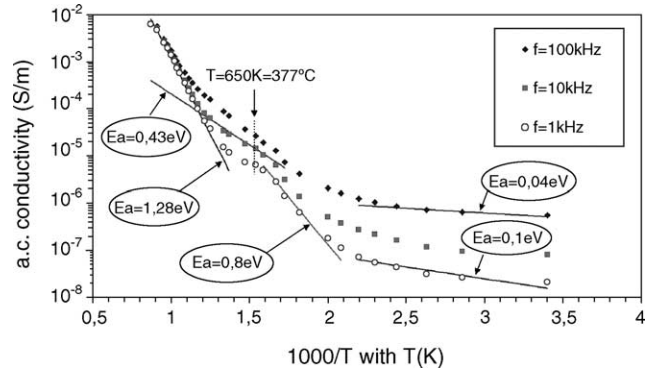


Fig. 5. Alternative conductivity in function of the reciprocal temperature at three frequencies (1, 10 and 100 kHz). The ac conductivity is given with a logarithmic scale. The points give the experimental values and the straight lines are simulation plots obtained with the indicated values of the activation energy as defined in Table 1.

very low value is in relation with a weak displacement of the electronic carriers. The very weak variations of the ϵ' permittivity and ac conductivity at temperatures below 230 °C are interesting properties for applications: for instance, this behaviour will guarantee the temperature stability of a resonator.

A first significant break of slope occurs towards 230 °C up to 377 °C (650 K). The most important variation is obtained at low frequency and gives an energy $E_{a3} = 0.8$ eV. A less strong slope is then observed up to 577 °C (850 K). This one gives an energy $E_{a4} = 0.43$ eV for $f = 10$ kHz. The four activation energies up to 577 °C (850 K) ($E_{a1} = 0.04$ eV, $E_{a2} = 0.1$ eV, $E_{a3} = 0.8$ eV and $E_{a4} = 0.43$ eV) are in relation with polaronic conduction based on the displacement of the electrons in the crystal lattice. Indeed, studies on titanates clearly highlight electronic conduction^{11–14} as these ceramics often can be oxygen deficient, due to the sintering under air or inadequate oxygen pressure, or due to impurities, which create acceptor levels that will be compensated by oxygen vacancies to establish the electric charges equilibrium. The highest value (0.8 eV) is recorded before the deformation observed towards 377 °C (650 K), and is so in relation with the plateau previously described on the evolution of losses. All the activation energies are recapitulated in Table 1 with the different temperature ranges.

Table 1

Activation energies of the La₂Ti₂O₇ ceramic in the 20–880 °C temperature range at different frequencies in relation with the ac conductivity plots (Fig. 5)

Temperature range (°C)	Frequency (kHz)	Activation energy (eV)
20–230	1	$E_{a1} = 0.1$
	100	$E_{a2} = 0.04$
230–377	1	$E_{a3} = 0.8$
377–577	1	Approximately 0.4
	10	$E_{a4} = 0.43$
577–880	1	$E_{a5} = 1.28$

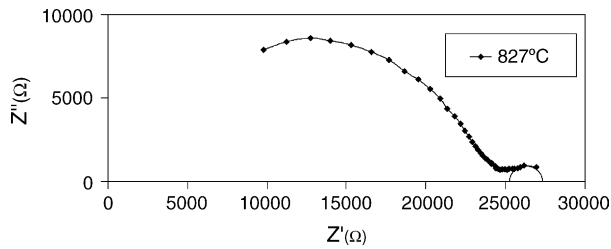


Fig. 6. Impedance diagram Z'' (Z') at high temperature (827°C) in the (1 kHz–1 MHz) frequency range. Z is the complex impedance of the sample.

Lastly, between 577°C (850 K) and 827°C (1100 K), the activation energy $E_{a5} = 1.28$ eV represents a conduction by displacement of the oxygen vacancies. This value a little higher than that obtained for lead zirconate titanate (PZT) or other titanates^{11–13} is nevertheless very close to that obtained on a $\text{La}_2\text{Ti}_2\text{O}_7$ ceramic¹⁵ where $E_a = 1.25$ eV. Fig. 6 presents the impedance diagram Z'' (Z') at high temperature ($827^\circ\text{C} = 1100$ K). The diagram is composed of two semi-circles representing the bulk and the ionic conductivity contributions. The small semi-circle, seen at low frequency, is due to the displacement of the oxygen vacancies. This phenomenon, observed at temperatures above 627°C (900 K), involves a creation of space charge by an accumulation of ionic carriers at the electrodes, which is a effect.

This ionic conduction allows to explain the strong variation of ε' shown in Fig. 3 at low frequency above 580°C . Indeed, the space charge capacity modifies the equivalent capacity of the sample and induces ε' drastically increases at frequencies below 20 kHz.

4. Conclusions

$\text{La}_2\text{Ti}_2\text{O}_7$ ceramic pellets have been synthesized and the dielectric properties have been characterized in a large frequency range from 100 Hz to 10 GHz, and in a large temperature range from 20 to 880°C . At low frequencies and room temperature, the permittivity ε' does not present dispersion and the loss tangent has a low value (1.6×10^{-3} at 100 kHz). A domain due to space charge has been found at about 1 GHz. The loss tangent increases drastically at high frequency. With measurements in our large temperature range, a Maxwell–Wagner effect was seen on the permittivity evolution at temperatures above 570°C . The study of the ac conductivity has allowed to calculate the activation energies for different mechanisms of carriers displacements. In par-

ticular for the oxygen vacancies, we have found $E_a = 1.28$ eV at 1 kHz.

It can be noted the lack of references available in the literature for the dielectric measurements on $\text{La}_2\text{Ti}_2\text{O}_7$ ceramic. The results obtained on bulk are promising for applications in electronics, in particular in microwaves on $\text{La}_2\text{Ti}_2\text{O}_7$ materials deposited in thin films.

References

- Kimura, M., Nanamatsu, S., Doi, K., Matsushita, S. and Takahashi, M., Electrooptic and piezoelectric properties of $\text{La}_2\text{Ti}_2\text{O}_7$ single crystal. *Jpn. J. Appl. Phys.*, 1972, **11**, 904.
- Nanamatsu, S., Kimura, M., Doi, K., Matsushita, S. and Yamada, N., A new ferroelectric: $\text{La}_2\text{Ti}_2\text{O}_7$. *Ferroelectrics*, 1974, **8**, 511–513.
- Takahashi, J., Kageyama, K. and Hayashi, T., Dielectric properties of double-oxide ceramics in the system $\text{Ln}_2\text{O}_3\text{--TiO}_2$ ($\text{Ln} = \text{La}, \text{Nd}$ and Sm). *Jpn. J. Appl. Phys.*, 1991, **30**, 2354.
- Takahashi, J., Kageyama, K. and Kodaira, K., Microwave dielectric properties of lanthanide titanate ceramics. *Jpn. J. Appl. Phys.*, 1993, **32**, 4327–4331.
- Le Gendre, L., Le Paven, C., Pinel, J., Fasquelle, D., Carru, J. C., Chevire, F., Tessier, F. and Marchand, R., Lanthanum titanium oxynitride thin films. *Silicates Ind.*, 2004, **69**(5–6), 165–171.
- Fuierer, P. A. and Newnham, R. E., $\text{La}_2\text{Ti}_2\text{O}_7$ ceramics. *J. Am. Ceram. Soc.*, 1991, **74**(11), 2876–2881.
- Fasquelle, D., Carru, J. C., Euphrasie, S., Pernod, P. and Daviero-Minaud, S., Hydrothermal synthesis of PbTiO_3 ferroelectric films. Characterization with large frequency and temperature ranges and sensor application. *Ferroelectrics*, 2003, **288**, 39.
- Fasquelle, D., Carru, J.-C., Duclère, J.-R., Guilloux-Viry, M., Le Gendre, L., Le Paven, C. et al., Caractérisations à large gamme de fréquences jusqu'à 10 GHz de matériaux ferroélectriques massifs et couche mince, 8ièmes. *Journées Caractérisations Microondes Matériaux (JCOMM 2004)*. La Rochelle, 31 mars–2 avril 2004.
- Bidault, O., Goux, P. and Maglione, M., Space charge relaxation in perovskites. *Phys. Rev. B*, 1994, **49**(12), 7868–7873.
- Ohi, K., Ishii, S. and Omura, H., Raman scattering study of incommensurate phase transitions in $\text{La}_2\text{Ti}_2\text{O}_7$. *Ferroelectrics*, 1992, **137**, 133–138.
- Ang, C., Yu, Z. and Cross, L. E., Oxygen-vacancy-related low frequency dielectric relaxation and electrical conduction in Si:SrTiO_3 . *Phys. Rev. B*, 2000, **62**(1), 228–236.
- Saha, S. and Krupanidhi, S. B., AC and DC Conductivity studies in pulsed laser ablated $(\text{Ba,Sr})\text{TiO}_3$ thin films. *Integr. Ferroelectr.*, 2001, **33**, 353–361.
- Saha, S. and Krupanidhi, S. B., Dielectric response in pulsed laser ablated $(\text{Ba,Sr})\text{TiO}_3$ thin films. *JAP*, 2000, **87**(2), 849–854.
- Smyth, D. M., defect structure in perovskite titanates. *Curr. Opin. Solid State Mater. Sci.*, 1996, **1**, 692–697.
- Takamura, H., Enomoto, K., Kamegawa, A. and Okada, M., Electrical conductivity of layered compounds in $\text{SrO--La}_2\text{O}_3\text{--TiO}_2$ systems prepared by the Pechini process. *Solid State Ionics*, 2002, **154/155**, 581–588.